ACS APPLIED MATERIALS & INTERFACES

Research Article

www.acsami.org

# Electron Beam Controlled Restructuring of Luminescence Centers in Polycrystalline Diamond

Cameron Zachreson, Aiden A. Martin, Igor Aharonovich,* and Milos Toth*

School of Physics and Advanced Materials, University of Technology, Sydney, Broadway, New South Wales 2007, Australia

**ABSTRACT:** Color centers in diamond are becoming prime candidates for applications in photonics and sensing. In this work we study the time evolution of cathodoluminescence (CL) emissions from color centers in a polycrystalline diamond film under electron irradiation. We demonstrate room-temperature activation of several luminescence centers through a thermal mechanism that is catalyzed by an electron beam. CL activation kinetics were measured in realtime and are discussed in the context of electron induced dehydrogenation of nitrogen-vacancy-hydrogen clusters and dislocation defects. Our results also show that (unintentional) electron beam induced chemical etching can take place during CL analysis of diamond. The etching is caused by residual $H_2O$ molecules present in high vacuum CL systems.

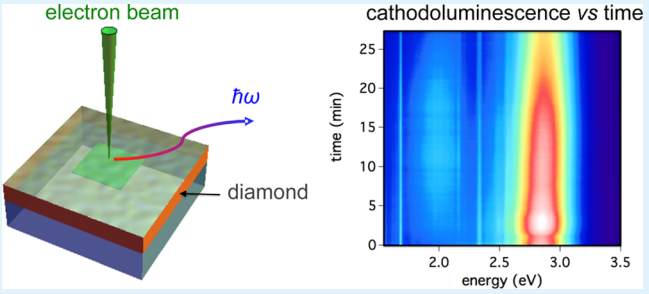


**KEYWORDS:** *diamond, nitrogen vacancy, dislocations, grain boundaries, cathodoluminescence, electron beam induced etching*

## 1. INTRODUCTION

Optical properties of materials, particularly of point defects in solids, are increasingly important to our understanding of single photon emitters. The negatively charged nitrogen vacancy (NV) center in diamond is an example of a color center that has been the subject of intense research because of its photophysical properties.[1−7] However, having a wide optical band gap, a diamond hosts many optically active defects and the interplay between them is still a subject of debate. The behavior of various color centers under electron beam irradiation has not been fully explored. An understanding of such phenomena will inform future work on deterministic, nanometer-scale processing of diamond-based devices, and may become useful in the context of biosensing and correlative microscopy.[8] Here we investigated the luminescence kinetics of several optical centers, including the nitrogen vacancy, in a polycrystalline diamond (PCD) film during exposure to 20 keV electrons.

The majority of prior work has focused on luminescence properties of single crystal diamonds that have undergone high-energy irradiation to add vacancies.[9−13] In our work, we study as-grown polycrystalline diamond that had not been subjected to ion-bombardment or annealing processes which are commonly used to induce the formation of nitrogen vacancy defects. The time evolution of cathodoluminescence (CL) spectra from a PCD film and several single crystal diamond control samples suggest that electron-catalyzed, thermally driven restructuring of extended defects activates luminescent NVs and A-band centers at room temperature, without the need for thermal annealing. The defect restructuring can be explained by electron beam induced dehydrogenation[14−17] of nonluminescent dislocations, and $NVH_x$ centers located at extended defects.

## 2. METHODS AND MATERIALS

A PCD thin film was deposited on a silicon substrate by microwave plasma-assisted chemical vapor deposition (MWCVD) using a microwave power of 900 W, a $H_2$:$CH_4$ ratio of 99:1, and a total pressure of 8 kPa. The film had a thickness of ∼400 nm and a grain size of ∼250 ± 50 nm. After synthesis, no further cleaning, annealing, or ion bombardment was performed. The sample was analyzed in the as-grown state.

Three single-crystal diamond samples were used for control experiments: a bulk CVD sample purchased from Element 6, a high-pressure high-temperature (HPHT) diamond (Sumitomo Inc.) and individual microdiamonds (Microdiamant). The HPHT diamond was sputter-coated with a 12 nm film of silver to suppress charging artifacts during CL analysis.

Cathodoluminescence characterization was carried out using an environmental scanning electron microscope (SEM)[18] with a base pressure of ∼$1 \times 10^{-4}$ Pa, equipped with a liquid nitrogen cooling stage. A parabolic mirror situated over the sample directed light through an ex situ focusing lens onto a 600 nm optical fiber coupled to a spectrometer (OceanOptics QE65000) with a bandpass of 6.5 nm. CL spectra were recorded continuously using an integration time of 10 s per spectrum while exposing a sample area of ∼20 $\mu m^2$ to 20 keV electrons using the beam currents shown in figure captions. The area sampled during CL analysis was significantly larger than the grain size of the PCD film. Hence, each data set reflects the mean response of a number of individual crystallites and grain boundaries. Each raw CL spectral kinetics profile was normalized and expressed as a color map (see Figures 2a and 3−5). A CL generation depth-profile (calculated

**Received:** March 27, 2014
**Accepted:** June 16, 2014
**Published:** June 16, 2014

  

using standard Monte Carlo techniques[19] for 20 keV electrons incident on a 400 nm diamond film on Si) is shown in Figure 1. The CL generation rate is approximated by the total energy deposition rate[20] (the dashed line shows the energy deposition depth profile in the substrate).

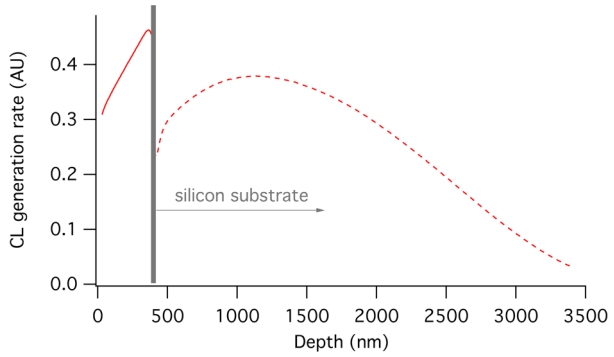


**Figure 1.** CL generation rate in diamond calculated as a function of depth for 20 keV electrons incident on a 400 nm diamond film on a silicon substrate. The dashed line shows the electron energy deposition depth profile in the substrate.

Individual CL kinetics profiles were obtained for the A-band and H3 emissions (attributed to dislocations, and nitrogen-vacancy complexes, respectively),[21] and the $NV^0$ emission from the PCD film. Figure 2b shows typical CL spectra and the corresponding peaks used to fit the three emissions, while Figure 2c shows the time evolution of the corresponding peak areas during electron irradiation. The silicon vacancy (SiV) emission at 1.68 eV and an emission at 2.56 eV were excluded from peak fitting because of their relatively small contributions to the total integrated intensity. In the PCD film, the H3 center was difficult to resolve individually because of peak overlaps. Hence, a sample of CVD microdiamonds showing only the H3 emission (Figure 5c) was measured and the resulting spectra fit to an exponentially modified Gaussian. The resulting coefficients were used to estimate the contribution of this defect to the PCD film emission spectrum. This method of H3 fitting is similar to that utilized by Tizei et al.[22,23]

## 3. RESULTS

The intensities of several luminescence centers varied with electron beam exposure time. We first characterized the CL kinetics measured from the PCD film under various ambient conditions. At room temperature, electron irradiation caused the $NV^0$ luminescence intensity to increase with time (Figure 3a). When residual water vapor was present in the high vacuum CL chamber, this initial increase was followed by a subsequent decrease with continued electron exposure (Figure 3a). However, when a liquid nitrogen cold trap was used to reduce the residual $H_2O$ pressure, the subsequent decrease was suppressed (Figure 3b). We note that in Figure 4, the cold trap appears to decrease the NV center activation rate. This effect is not real, and is a consequence of the fact that each spectral CL kinetics profile was normalized (in order to show clearly the changes in each data set). The absolute change in $NV^0$ intensity seen in Figure 4b is much greater than the corresponding change in Figure 4a. Conversely, when the water vapor pressure was increased to 47 Pa,[18] the intensity of all CL emissions rapidly decreased with irradiation time (Figure 3c).

The A-band luminescence exhibited two general trends during electron irradiation of different regions of the PCD film. The signal intensity would either decrease with exposure time (Figure 2), or an initial increase in intensity was followed by an

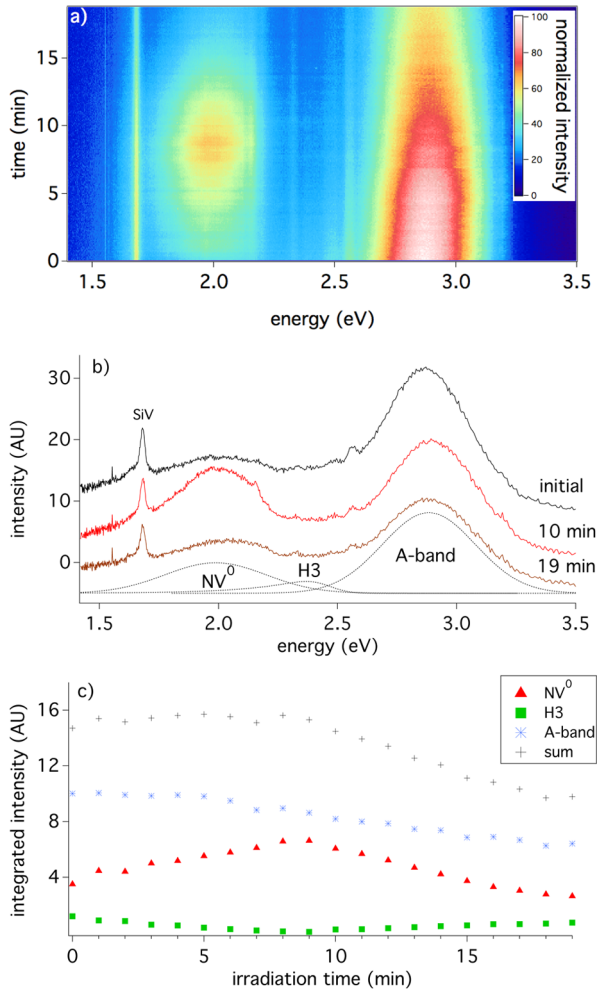


**Figure 2.** CL kinetics profiles recorded from a PCD film during a 20 min electron beam irradiation treatment: (a) a normalized color map representation of CL spectra acquired as a function of time; (b) corresponding CL spectra at electron exposure times of 0, 10, and 19 min; and (c) time-evolution of the A-band, $NV^0$, and H3 emissions, plotted as the area of each of the peaks shown in b versus time. (Beam current = 23 nA.)

eventual decay (Figures 3a, b and 4b). We attribute this variability accross the PCD surface to a nonuniform distribution of the $sp^2$ species associated with dislocations responsible for A-band luminescence[21,24] in the as-grown PCD film, and variations in the number of grain boundaries within the probed volume. All other trends in CL kinetics profiles reported here for the polycrystalline sample were observed in multiple locations and did not vary across the PCD film.

To characterize the effects of sample temperature, we measured CL kinetics at −25 °C and −177 °C (Figure 4). Sample cooling to −25 °C reduced the magnitude of the electron beam induced increase in the intensity of the $NV^0$ CL emission. At −177 °C, the effect was suppressed to below the detection limit and the entire CL spectrum decayed with electron exposure time. The rapid decay of all CL emissions seen in Figure 4a is attributed to electron beam induced etching, accelerated by a high coverage of $H_2O$ molecules at the cold diamond surface.

Figure 5 shows reference data collected at room temperature from single crystal control samples, each containing only one of the three CL emissions of interest: (a) bulk CVD diamond

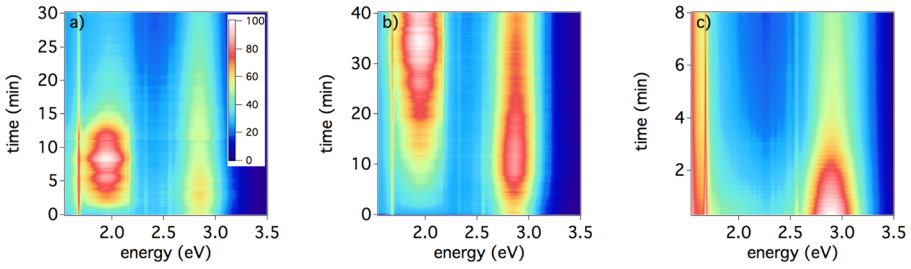


**Figure 3.** CL kinetics profiles obtained from a PCD film under the following conditions of temperature and humidity: (a) room temperature with no measure taken to remove residual water molecules from a high vacuum CL analysis chamber, (b) room temperature with an in-chamber liquid nitrogen-cooled trap used to cryo pump residual water vapor, and (c) room temperature with a water vapor pressure of 47 Pa. (Beam current = (a) 52 and (b, c) 43 nA.)

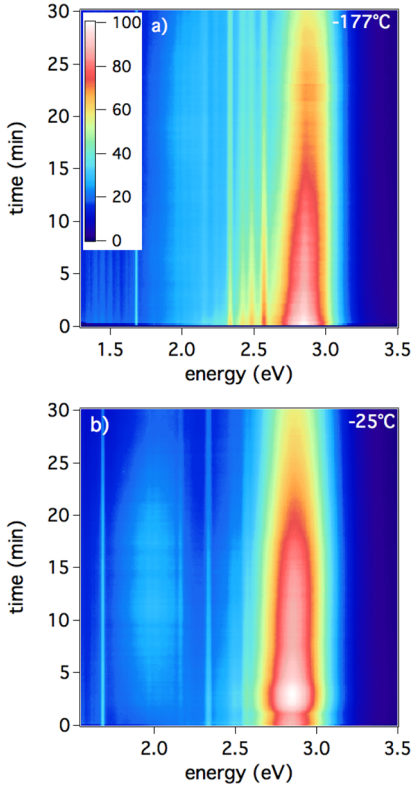


**Figure 4.** CL kinetics profiles obtained from a PCD film cooled to (a) −177 °C, and (b) −25 °C. (Beam current = (a) 33 and (b) 52 nA.)

enriched with NV centers, (b) HPHT diamond that exhibits A-band luminescence, and (c) a single microdiamond that contains H3 centers. In a single-crystal diamond (i.e., in the absence of grain boundaries), the $NV^0$ emission did not change with electron exposure time (Figure 5a). The A-band intensity shows an increase with irradiation time (Figure 5b), but the eventual decrease in A-band intensity observed in the PCD film was not observed in the bulk, single-crystal diamond, because of negligible electron beam-induced etching (see Discussion) of the bulk diamond relative to that of the polycrystalline film. The H3 emission intensity exhibits an initial decrease followed by an increase with time in both single-crystal microdiamonds (Figure 5c) and the PCD film (Figure 2c). These results show that the H3 kinetics can occur in the absence of $NV^0$ kinetics, and are therefore not necessarily the consequence of competitive recombination. We note that, in Figure 5c, the narrow line at 1.4 eV is associated with a Ni-related defect[21,25,26] and decreases marginally with electron exposure. It serves as an internal control, showing that the change in H3 CL intensity with irradiation time is not caused by an experimental artifact such as beam drift or fluctuations in beam current.

In all cases, the intensity of the SiV emission in the PCD film decreased with electron irradiation time, as seen in Figure 2b (the apparent increase seen in 3 is caused by an overlap between the SiV and $NV^0$ peaks). While uninteresting in isolation, this behavior acts as an effective control for experimental artifacts, analogous to the aforementioned Ni defect in the microdiamond.

## 4. DISCUSSION

We now discuss possible mechanisms behind the changes in luminescence caused by electron irradiation of the PCD film. In particular, we focus on the initial increase in the $NV^0$ and A-band intensity, and the eventual decay of most emissions caused by prolonged electron exposure. The latter is attributed

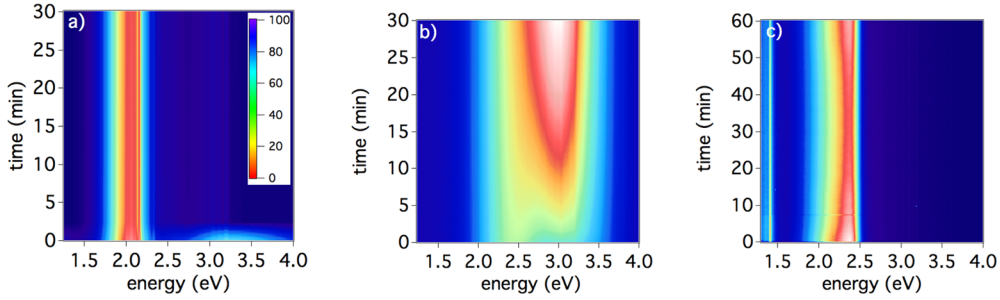


**Figure 5.** CL kinetics profiles recorded from control samples that exhibit specific luminescent features: (a) bulk CVD single-crystal diamond showing $NV^0$ luminescence, (b) HPHT single-crystal diamond showing A-band luminescence, (c) single microdiamond showing H3 luminescence. (Beam current = (a, b) 45 and (c) 3 nA.)


dx.doi.org/10.1021/am501865t | ACS Appl. Mater. Interfaces 2014, 6, 10367−10372

primarily to efficient electron beam induced etching (EBIE) of polycrystalline diamond,[27−31] mediated by residual $H_2O$ molecules present in the high vacuum SEM chamber[32] used for CL analysis. EBIE is a dry etch process that proceeds through electron induced dissociation of surface adsorbed precursor molecules (in this case $H_2O$). Dissociation yields fragments (e.g., O radicals) that react with the surface, producing volatile species (e.g., CO) that desorb from and thereby etch the substrate.[33,34] The most direct evidence for the role of EBIE in CL kinetics is shown in Figure 3b, where a liquid nitrogen cold trap was used to reduce the residual $H_2O$ pressure in the high vacuum CL analysis chamber. The cold trap was not in contact with the sample, but nonetheless caused a significant reduction in the long term decay rate of most emissions (SiV, $NV^0$ and A-band) present in the PCD CL spectrum. Conversely, when the water vapor pressure was increased to 47 Pa (in the absence of a cold trap; Figure 3c), the CL decay rates increased dramatically, resulting in rapid quenching of the entire CL spectrum with electron irradiation time. Furthermore, in this extreme case, an etch pit was clearly visible in electron images of the sample region that had been irradiated by the electron beam. The correlation between $H_2O$ pressure and the CL decay rate is consistent with EBIE because the etch rate scales with precursor adsorbate coverage[28,33] at the diamond surface.

The long-term decay of CL emissions ascribed to EBIE is not evident in CL kinetics profiles acquired from bulk, single crystal diamond samples (Figure 5a, b). We attribute this to the fact that the EBIE rate of polycrystalline diamond is greater than that of the single-crystal diamond[27,28] (i.e., etching is most efficient at grain boundaries), and that etching has no significant effect on the thickness of the bulk, single crystal diamond. We note that when the etch rate is low (as in the case of single crystal diamond), etching can be terminated entirely by a competing process of contamination buildup under the electron beam caused by electron induced decomposition of hydrocarbon contaminants that are present in most vacuum systems.[32,35]

The long-term decay of CL emissions ascribed to EBIE is also not evident in the H3 CL kinetics profiles acquired from the PCD film (Figure 2b) and the microdiamond (Figure 5c). In both cases, the H3 CL intensity exhibits an initial decrease followed by an increase with irradiation time, even when etching was observed in electron images taken after electron exposure. The mechanism behind the increase in H3 CL intensity is not understood.

We now turn to the initial increase in $NV^0$ and A-band CL emission intensities with electron exposure time (see, for example, Figure 3a, b). First, we exclude a number of potential mechanisms that cannot explain our results. The electron beam energy (of 20 keV) was well below the threshold for knock-on generation of vacancy-interstitial pairs in bulk diamond.[36,37] Direct generation of vacancies in bulk diamond (through knock-on or electron excitation mechanisms[15,38−41]) is also inconsistent with the data presented in Figure 5b. Such a process is expected to create NV centers in HPHT diamond which contains nitrogen impurities but few vacancies. Similarly, nitrogen diffusion within or into bulk diamond is not supported by our data, which show no indication of a direct relationship between the $NV^0$ and H3 emissions (H3 centers are associated with nitrogen aggregates[21]), and no change in the $NV^0$ emission intensity in single crystal diamond.

Electron induced dissociation of residual $H_2O$ adsorbates can, in principle, give rise to oxidation[42] of as-grown, H-terminated diamond surfaces. A change in surface termination from H to O has been shown to switch the charge state of near-surface $NV^0$ centers, causing an increase the ratio of $NV^-$ to $NV^0$ centers.[43,44] However, this effect cannot explain the increase in $NV^0$ intensity reported here because the $NV^-$ emission is invisible in CL spectra. Hence, if this process dominated CL kinetics, we would expect a decrease rather than an increase in $NV^0$ intensity with electron exposure time.

Electron beam heating is negligible[13] because of the high thermal conductivity of diamond, and good thermal contact between the PCD diamond film, the Si substrate and the specimen holder.

The last mechanism that we exclude as the cause of the observed CL kinetics is electromigration[45−48] of point defects in the PCD film. The temperature dependencies seen in Figure 4 show that sample cooling suppressed the magnitudes of the increase in the $NV^0$ and A-band CL intensities. This behavior is the opposite of that expected for electromigration (since thermal detrapping suppresses the charging effects that cause electromigration[45−48]). Charging effects were minimized by the use of a 20 keV electron beam. The electron range was ∼3.5 $\mu$m, and the beam therefore penetrated through the 400 nm PCD film, into the conductive Si substrate (see Figure 1. The observed temperature dependencies, however, are consistent with thermal restructuring or diffusion of defects in the sample. We therefore suggest that electron beam catalyzed, thermally driven dehydrogenation activates NV and A-band luminescence centers, noting that

- We expect hydrogen to be present at the grain boundaries and dislocations of the as-grown PCD film, because of the nature of the CVD growth process.[49,50]
- Introduction of hydrogen into a sample containing bright NV centers has been shown to quench NV luminescence.[51]
- The A-band luminescence originates from certain types of dislocations[21] and has been associated with $sp^2$ carbon,[24] which can form upon hydrogen desorption due to the restructuring of dangling bonds.[52]

Removal of hydrogen from $NVH_x$ centers located at or near grain boundaries, and from nonluminescent dislocations is the simplest explanation that is consistent with our CL data, and the aforementioned literature. Electron irradiation likely lowers the energy barrier for thermal dissociation of the hydrogenated complexes, thereby catalyzing the dehydrogenation process.

It is well-known that electron beam irradiation in an SEM (and electron injection by a scanning tunneling microscope) can give rise to the dissociation of hydrogenated complexes in several materials.[53−57] In the case of diamond, the dissociation kinetics of boron−hydrogen and boron−deuterium complexes have been characterized by CL analysis, and ascribed primarily to cumulative vibrational (rather than electronic) excitation,[14−17] a process whose efficiency scales inversely with temperature.[17] In contrast, the CL activation process reported here is suppressed by cooling, indicating a different excitation pathway. The data cannot, however, be used to deduce the exact nature of the excitation mechanism.

## 5. CONCLUSIONS

To summarize, we observed CL kinetics in a PCD film irradiated by a 20 keV electron beam. The intensities of $NV^0$, A-

band, H3, and SiV CL emissions were shown to change with time. To explain the increases in the intensities of $NV^0$ and A-band emissions, we propose electron beam induced dehydrogenation of CL centers at dislocations and grain boundaries as a possible mechanism. Our results also show that CL emissions from diamond can be quenched by electron beam induced etching caused by $H_2O$ molecules present in high vacuum CL chambers. This effect is generally undesirable and can be suppressed by minimizing the partial pressure of residual $H_2O$.

## AUTHOR INFORMATION


### Corresponding Authors

*E-mail: Igor.Aharonovich@uts.edu.au.
*E-mail: Milos.Toth@uts.edu.au.


### Notes

The authors declare no competing financial interest.

## ACKNOWLEDGMENTS

We are grateful to Steven Prawer and Mark Newton for useful discussions. This work was supported by FEI Company and the Australian Research Council (Project DP140102721). A.A.M. is the recipient of a John Stocker Postgraduate Scholarship from the Science and Industry Endowment Fund. I.A. is the recipient of an Australian Research Council Discovery Early Career Research Award (Project DE130100592).

## REFERENCES


(1) Doherty, M. W.; Manson, N. B.; Delaney, P.; Jelezko, F.; Wrachtrup, J.; Hollenberg, L. C. The Nitrogen-Vacancy Colour Centre in Diamond. *Phys. Rep.* **2013**, *528*, 1−45.

(2) Childress, L.; Hanson, R. Diamond NV Centers for Quantum Computing and Quantum Networks. *MRS Bull.* **2013**, *38*, 134−138.

(3) Dobrovitski, V.; Fuchs, G.; Falk, A.; Santori, C.; Awschalom, D. Quantum Control over Single Spins in Diamond. *Annu. Rev. Condens. Matter Phys.* **2013**, *4*, 23−50.

(4) Hausmann, B. J.; Shields, B. J.; Quan, Q.; Chu, Y.; de Leon, N. P.; Evans, R.; Burek, M. J.; Zibrov, A. S.; Markham, M.; Twitchen, D. J.; Park, H.; Lukin, M. D.; Loncar, M. Coupling of NV Centers to Photonic Crystal Nanobeams in Diamond. *Nano Lett.* **2013**, *13*, 5791−5796.

(5) Wrachtrup, J.; Jelezko, F.; Grotz, B.; McGuinness, L. Nitrogen-Vacancy Centers Close to Surfaces. *MRS Bull.* **2013**, *38*, 149−154.

(6) Grotz, B.; Hauf, M. V.; Dankerl, M.; Naydenov, B.; Pezzagna, S.; Meijer, J.; Jelezko, F.; Wrachtrup, J.; Stutzmann, M.; Reinhard, F.; Garrido, J. A. Charge State Manipulation of Qubits in Diamond. *Nat. Commun.* **2012**, *3*, 729.

(7) Aharonovich, I.; Greentree, A. D.; Prawer, S. Diamond Photonics. *Nat. Photonics* **2011**, *5*, 397−405.

(8) Modla, S.; Czymmek, K. J. Correlative Microscopy: A Powerful Tool for Exploring Neurological Cells and Tissues. *Micron* **2011**, *42*, 773−792.

(9) Robins, L.; Cook, L.; Farabaugh, E.; Feldman, A. Cathodoluminescence of Defects in Diamond Films and Particles Grown by Hot-Filament Chemical-Vapor Deposition. *Phys. Rev. B: Condens. Matter Mater. Phys.* **1989**, *39*, 13367−13377.

(10) Davies, G. Dynamic Jahn-Teller Distortions at Trigonal Optical Centres in Diamond. *J. Phys. C: Solid State Phys.* **1979**, *12*, 2551−2556.

(11) Martin, J.; Wannemacher, R.; Teichert, J.; Bischoff, L.; Kohler, B. Generation and Detection of Fluorescent Color Centers in Diamond with Submicron Resolution. *Appl. Phys. Lett.* **1999**, *75*, 3096−3098.

(12) Martin, J.; Grebner, W.; Sigle, W.; Wannemacher, R. Confocal Microscopy of Color Center Distributions in Diamond. *J. Lumin.* **1999**, *83*, 493−497.

(13) Schwartz, J.; Aloni, S.; Ogletree, D. F.; Schenkel, T. Effects of Low-Energy Electron Irradiation on Formation of Nitrogen-Vacancy Centers in Single-Crystal Diamond. *New J. Phys.* **2012**, *14*, 043024.

(14) Barjon, J.; Chevallier, J.; Jomard, F.; Baron, C.; Deneuville, A. Electron-Beam-Induced Dissociation of B-D Complexes in Diamond. *Appl. Phys. Lett.* **2006**, *89*, 232111.

(15) Barjon, J.; Mehdaoui, A.; Jomard, F.; Chevallier, J.; Mer, C.; Nesladek, M.; Bergonzo, P.; Pernot, J.; Omnes, F.; Deneuville, A. Stability of B-H and B-D Complexes in Diamond Under Electron Beam Excitation. *Appl. Phys. Lett.* **2008**, *93*, 062108.

(16) Goss, J.; Briddon, P. Dissociation of B−H Pairs in Diamond as Enhanced by Electronic Excitation and Electron Capture: Computational Modeling. *Phys. Rev. B: Condens. Matter Mater. Phys.* **2008**, *77*, 035211.

(17) Habka, N.; Chevallier, J.; Barjon, J. Electron-Beam-Induced Dissociation of (B,D) Complexes in Diamond Mediated by Multiple Vibrational Excitations. *Phys. Rev. B: Condens. Matter Mater. Phys.* **2010**, *81*, 045207.

(18) Danilatos, G. D. Foundations of Environmental Scanning Electron Microscopy. *Adv. Electron. Electron Phys.* **1988**, *71*, 109−250.

(19) Hovington, P.; Drouin, D.; Gauvin, R. CASINO: A New Monte Carlo Code in C Language for Electron Beam Interaction 0.1. Description of the Program. *Scanning* **1997**, *19*, 1−14.

(20) Toth, M.; Phillips, M. R. Monte Carlo Modeling of Cathodoluminescence Generation using Electron Energy Loss Curves. *Scanning* **1998**, *20*, 425−432.

(21) Zaitsev, A. M. *Optical Properties of Diamond: A Data Handbook*; Springer-Verlag: Berlin, 2001.

(22) Tizei, L. H. G.; Meuret, S.; Nagarajan, S.; Treussart, F.; Fang, C.-Y.; Chang, H.-C.; Kociak, M. Spatially and Spectrally Resolved Cathodoluminescence with Fast Electrons: A Tool for Background Subtraction in Luminescence Intensity Second-Order Correlation Measurements Applied to Subwavelength Inhomogeneous Diamond Nanocrystals. *Phys. Status Solidi A* **2013**, *210*, 2060−2065.

(23) Tizei, L.; Kociak, M. Spectrally and Spatially Resolved Cathodoluminescence of Nanodiamonds: Local Variations of the $NV^0$ Emission Properties. *Nanotechnology* **2012**, *23*, 175702.

(24) Takeuchi, D.; Watanabe, H.; Yamanaka, S.; Okushi, H.; Sawada, H.; Ichinose, H.; Sekiguchi, T.; Kajimura, K. Origin of Band-A Emission in Diamond Thin Films. *Phys. Rev. B: Condens. Matter Mater. Phys.* **2001**, *63*, 245328.

(25) Orwa, J.; Aharonovich, I.; Jelezko, F.; Balasubramanian, G.; Balog, P.; Markham, M.; Twitchen, D.; Greentree, A.; Prawer, S. Nickel Related Optical Centres in Diamond Created by Ion Implantation. *J. Appl. Phys.* **2010**, *107*, 093512.

(26) Kupriyanov, I.; Gusev, V.; Borzdov, Y. M.; Kalinin, A.; Pal'Yanov, Y. N. Photoluminescence Study of Annealed Nickel- and Nitrogen-Containing Synthetic Diamond. *Diamond Relat. Mater.* **1999**, *8*, 1301−1309.

(27) Martin, A. A.; Toth, M.; Aharonovich, I. Subtractive 3D Printing of Optically Active Diamond Structures. *Sci. Rep.* **2014**, *4*, 5022.

(28) Martin, A. A.; Phillips, M. R.; Toth, M. Dynamic Surface Site Activation: A Rate Limiting Process in Electron Beam Induced Etching. *ACS Appl. Mater. Interfaces* **2013**, *5*, 8002−8007.

(29) Taniguchi, J.; Miyamoto, I.; Ohno, N.; Honda, S. Electron Beam Assisted Chemical Etching of Single Crystal Diamond Substrates. *Jpn. J. Appl. Phys.* **1996**, *35*, 6574−6578.

(30) Taniguchi, J.; Miyamoto, I.; Ohno, N.; Kantani, K.; Komuro, M.; Hiroshima, H. Electron Beam Assisted Chemical Etching of Single-Crystal Diamond Substrates with Hydrogen Gas. *Jpn. J. Appl. Phys.* **1997**, *36*, 7691−7695.

(31) Niitsuma, J.-i.; Yuan, X.-l.; Koizumi, S.; Sekiguchi, T. Nanoprocessing of Diamond Using a Variable Pressure Scanning Electron Microscope. *Jpn. J. Appl. Phys.* **2006**, *45*, L71−L73.

(32) Lobo, C. J.; Martin, A.; Phillips, M. R.; Toth, M. Electron Beam Induced Chemical Dry Etching and Imaging in Gaseous $NH_3$ Environments. *Nanotechnology* **2012**, *23*, 375302.

(33) Utke, I.; Moshkalev, S.; Russell, P. *Nanofabrication Using Focused Ion and Electron Beams: Principles and Applications*; Oxford University Press: New York, 2012.
(34) Arumainayagam, C. R.; Lee, H.-L.; Nelson, R. B.; Haines, D. R.; Gunawardane, R. P. Low-Energy Electron-Induced Reactions in Condensed Matter. *Surf. Sci. Rep.* **2010**, *65*, 1−44.
(35) Toth, M.; Lobo, C. J.; Hartigan, G.; Knowles, W. R. Electron Flux Controlled Switching Between Electron Beam Induced Etching and Deposition. *J. Appl. Phys.* **2007**, *101*, 054309.
(36) Campbell, B.; Mainwood, A. Radiation Damage of Diamond by Electron and Gamma Irradiation. *Phys. Status Solidi A* **2000**, *181*, 99−107.
(37) Koike, J.; Parkin, D. M.; Mitchell, T. E. Displacement Threshold Energy for Type IIa Diamond. *Appl. Phys. Lett.* **1992**, *60*, 1450−1452.
(38) Banhart, F. Irradiation Effects in Carbon Nanostructures. *Rep. Prog. Phys.* **1999**, *62*, 1181−1221.
(39) Egerton, R. F.; Li, P.; Malac, M. Radiation Damage in the TEM and SEM. *Micron* **2004**, *35*, 399−409.
(40) Krasheninnikov, A. V.; Nordlund, K. Ion and Electron Irradiation-Induced Effects in Nanostructured Materials. *J. Appl. Phys.* **2010**, *107*, 071301.
(41) Krasheninnikov, A. V.; Banhart, F. Engineering of Nanostructured Carbon Materials with Electron or Ion Beams. *Nat. Mater.* **2007**, *6*, 723−733.
(42) Toth, M.; Lobo, C. J.; Lysaght, M. J.; Vladar, A. E.; Postek, M. T. Contamination-Free Imaging by Electron Induced Carbon Volatilization in Environmental Scanning Electron Microscopy. *J. Appl. Phys.* **2009**, *106*, 034306.
(43) Fu, K.-M.; Santori, C.; Barclay, P.; Beausoleil, R. Conversion of Neutral Nitrogen-Vacancy Centers to Negatively Charged Nitrogen-Vacancy Centers Through Selective Oxidation. *Appl. Phys. Lett.* **2010**, *96*, 121907.
(44) Rondin, L.; Dantelle, G.; Slablab, A.; Grosshans, F.; Treussart, F.; Bergonzo, P.; Perruchas, S.; Gacoin, T.; Chaigneau, M.; Chang, H. C.; Jacques, V.; Roch, J. F. Surface-Induced Charge State Conversion of Nitrogen-Vacancy Defects in Nanodiamonds. *Phys. Rev. B: Condens. Matter Mater. Phys.* **2010**, *82*, 115449.
(45) Cazaux, J. Scenario for Time Evolution of Insulator Charging Under Various Focused Electron Irradiations. *J. Appl. Phys.* **2004**, *95*, 731−742.
(46) Cazaux, J. About the Charge Compensation of Insulating Samples in XPS. *J. Electron Spectrosc. Relat. Phenom.* **2000**, *113*, 15−33.
(47) Cazaux, J. Mechanisms of Charging in Electron Spectroscopy. *J. Electron Spectrosc. Relat. Phenom.* **1999**, *105*, 155−185.
(48) Cazaux, J. Charging in Scanning Electron Microscopy "From Inside and Outside". *Scanning* **2004**, *26*, 181−203.
(49) Ballutaud, D.; Jomard, F.; Theys, B.; Mer, C.; Tromson, D.; Bergonzo, P. Hydrogen Diffusion and Stability in Polycrystalline CVD Undoped Diamond. *Diamond Relat. Mater.* **2001**, *10*, 405−410.
(50) Ballutaud, D.; Simon, N.; Girard, H.; Rzepka, E.; Bouchet-Fabre, B. Photoelectron Spectroscopy of Hydrogen at the Polycrystalline Diamond Surface. *Diamond Relat. Mater.* **2006**, *15*, 716−719.
(51) Stacey, A.; Karle, T.; McGuinness, L.; Gibson, B.; Ganesan, K.; Tomljenovic-Hanic, S.; Greentree, A.; Hoffman, A.; Beausoleil, R.; Prawer, S. Depletion of Nitrogen-Vacancy Color Centers in Diamond via Hydrogen Passivation. *Appl. Phys. Lett.* **2012**, *100*, 071902.
(52) Laikhtman, A.; Hoffman, A. Synchrotron Radiation Study of Surface Versus Sub-Surface Deuterium in Diamond Films Produced by Exposure to Deuterium Activated by Hot Filament-High Vacuum and Ex Situ Microwave Plasma. *Diamond Relat. Mater.* **2002**, *11*, 371−377.
(53) Becker, R. S.; Higashi, G. S.; Chabal, Y. J.; Becker, A. J. Atomic-Scale Conversion of Clean Si (111): H-1 1 to Si (111)-2 1 by Electron-Stimulated Desorption. *Phys. Rev. Lett.* **1990**, *65*, 1917−1920.
(54) Foley, E. T.; Kam, A. F.; Lyding, J. W.; Avouris, P. Cryogenic UHV-STM Study of Hydrogen and Deuterium Desorption from Si(100). *Phys. Rev. Lett.* **1998**, *80*, 1336−1339.
(55) Li, X.; Coleman, J. J. Time-Dependent Study of Low Energy Electron Beam Irradiation of Mg-Doped GaN Grown by Metalorganic Chemical Vapor Deposition. *Appl. Phys. Lett.* **1996**, *69*, 1605−1607.
(56) Shen, T.-C.; Wang, C.; Abeln, G. C.; Tucker, J. R.; Lyding, J. W.; Avouris, P.; Walkup, R. E. Atomic-Scale Desorption Through Electronic and Vibrational Excitation Mechanisms. *Science* **1995**, *268*, 1590−1592.
(57) Silvestre, S.; Bernard-Loridant, D.; Constant, E.; Constant, M.; Chevallier, J. Electron-Beam-Induced Reactivation of Si Dopants in Hydrogenated GaAs: A Minority Carrier Generation Effect or an Energetic Electron Excitation Effect? *Appl. Phys. Lett.* **2000**, *77*, 3206−3208.